International Forum on Aeroelasticity and Structural Dynamics
IFASD 2024
17-21 June 2024, The Hague, The Netherlands

MACHINE LEARNING TO FORECAST UNSTEADY, MOTION-INDUCED UNSTEADY FORCES

Reik Thormann[1] **and Hans M. Bleecke**[1]

[1]Airbus Operations
Airbus Allee 1, 28199 Bremen, Germany
reik.thormann@airbus.com

Keywords: Machine learning, unsteady aerodynamics, flutter, high-aspect-ratio wing

Abstract: In this paper, the combination of an auto-encoder coupled with a transformer is presented to predict unsteady surface pressures due to forced excitation. While the used neural-network architecture operates in the the time domain, training data are computed with the linearized, frequency-domain CFD solver for a generic, high-aspect-ratio wing. These data are transfered into the time-domain to train the network, while the network's outputs are Fourier transformed and compared to their corresponding reference. Results are compared for unsteady, local surface pressures, frequency response functions of the generalized aerodynamic force matrices as well as flutter predictions.

1 INTRODUCTION

Through the advancements in computational technology and numerical methods over the last decades, high-fidelity computational fluid dynamics (CFD) analysis are nowadays well established in industrial problems. Despite these advancements, however, high-fidelity CFD aerodynamics is still very expensive and as such a bottleneck to applications in many aeroelastic problems. Model-order reduction and Machine Learning (ML) techniques are a means to reduce the cost of high-fidelity CFD analyses by constructing models with appropriate accuracy and lower computational complexity.

In a collaboration project with University of Michigan (2018-2022), first steps were made in developing and applying interpolation and projection based model-order reduction methods, [1], [2]. The ambition of applying ML techniques is the detection of critical flutter speeds with lower computational costs. This should cover the entire flight envelope for all load conditions, including flexible wings with high-aspect-ratios, thus contributing to the safety of aircraft designs.

In [3], DLR succesfully showed an approach based on proper orthogonal decomposition and autoencoder feed-forward neural networks, implemented in their SMARTy toolbox [4] and applied to the construction of a data-driven unsteady reduced order model for the prediction of aerodynamic relevant variables for both field quantities and integral coefficients for a two-dimensional pitching and plunging airfoil.

The present work focuses on the use of data-driven neural networks based on the nonlinear autoencoder reduction method coupled to the more recent transformer technique [5] to predict forced-motion unsteady aerodynamic pressure responses and its applicability to determine the flutter speeds of a high-aspect-ratio wing in comparison to the flutter speeds based on the reference TAU-LFD method, [6].

2 METHODS

2.1 Auto-Encoder

While the Proper Orthogonal Decomposition (POD) provides a good compression rate while retaining accuracy for linear data, it quickly reaches its limits for nonlinear training data. Therefore, the nonlinear reduction method "Auto-Encoder" is employed to have a better trade-off between size of the latent space and compression loss. A sketch of an auto-encoder is given

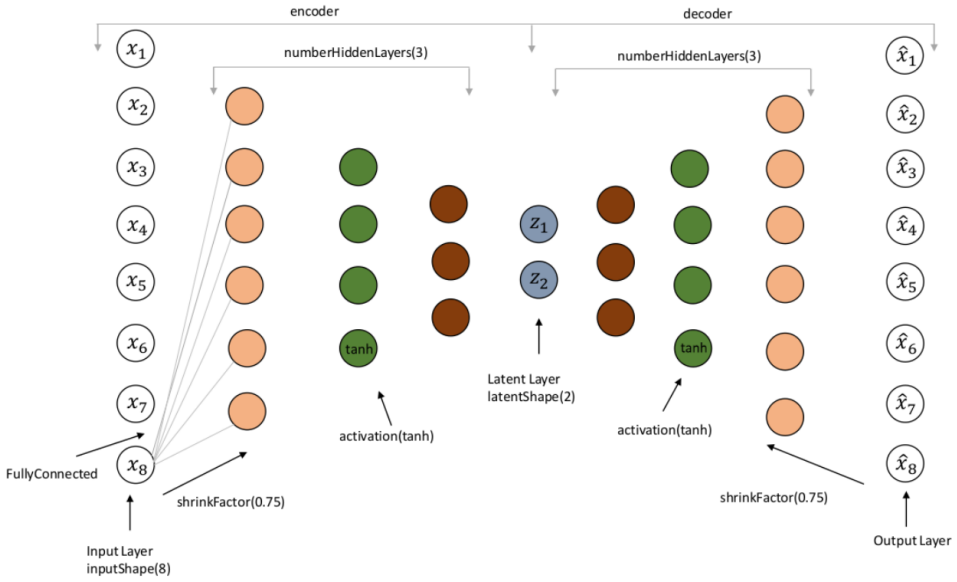

Figure 1: Sketch for AutoEncoder from SMARTy [4] user-guide

in Figure 1. The encoder consists of several fully-connected linear layers where the number of inputs is larger than the number of outputs to subsequently reduce the dimension of the latent space. Between each layer, an activation function, e.g. "ReLu" or "Tanh", is called to introduce nonlinearity into the neural network. The decoder has usually the same setup as the encoder but in reversed order. The encoder and decoder are trained simultaneously, so that the input to the encoder must be the output of the decoder. In this paper, the loss function during training was modified. Instead of using the mean-square error directly on the c_p values, they are scaled by their associated surface area to guide the optimizer and regularize the latent space. The auto-encoder is parameterized via the size of the latent space - i.e. the size of the encoder output - and via the shrink factor in each layer.

2.2 Transformer

Once the auto-encoder is formed, another neural network is required to link the excitation to the response inside the latent space. While recurrent neural networks like LSTM and GRU could perform such time integrations, a more recent technique called transformer [5] is used in this paper.

The setup of the neural network, see Figure 2, is split into two parts: encoder(left) and decoder (right). Even though it is denoted similarly to the auto-encoder parts, there is no relation between them. Each of them starts with a linear layer followed by positional encoding which can be interpreted as a wavelet transformation. Afterwards, several layers of so-called self-attention layers are used followed by a linear feed-forward layer for the decoder giving the final output of this neural network. In this paper, the inputs to the transformer are the modal displacements,

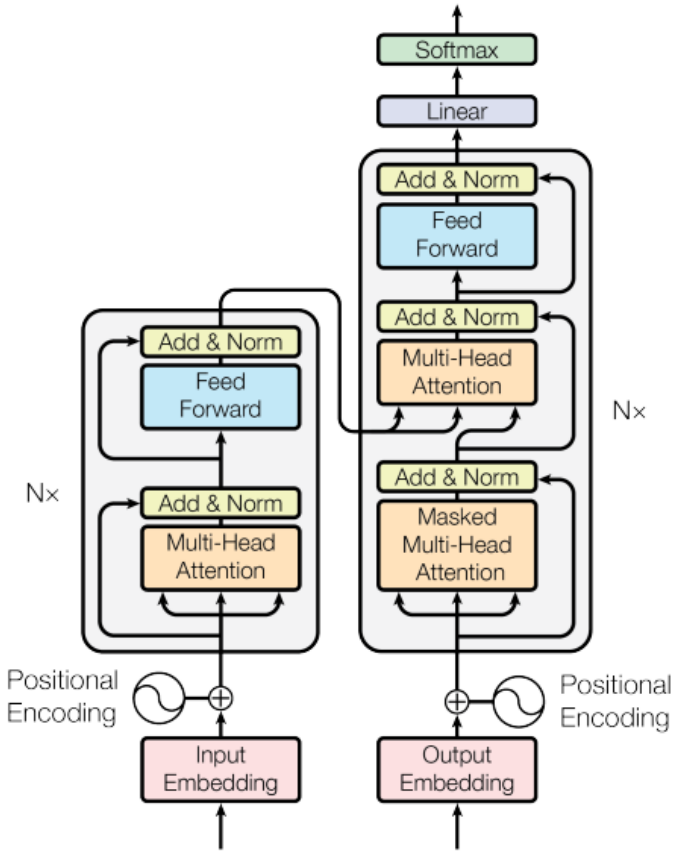

Figure 2: Sketch for Transformer [5]

velocity and acceleration of the current time step and of N_{old} previous time steps. The output is the vector of the encoded c_p of the current time step.

3 TEST CASE

3.1 Configuration

The capabilities of the neural networks are demonstrated on a generic, high-aspect-ratio wing, see Figure 3 for the CFD and FE model. The structural model is clamped at the symmetry plane and the first twelve modes are considered during the flutter analysis. The list of mode names is given in Table 1 and the overview of flow parameter is given in Table 2.

3.2 Aerodynamic model

The DLR TAU-code [7] is used to solve the steady and the unsteady Reynolds Averaged Navier Stokes (URANS) equations in combination with the Spalart-Allmaras model [8]. The solver is based on a finite volume scheme on unstructured grids.

At first, for the current flight point (Mach number, angle of attack, speed combination), a steady CFD-CSM coupled simulation is performed following the process described in [9]. Around this aeroelastic equilibrium, unsteady simulations are performed using the linear-frequency domain (LFD) solver [6] to generate training and test data. LFD computations are performed for all 12 modes at reduced frequencies $\omega^* = [0.02, 0.05, 0.1, 0.15, 0.2, 0.25, 0.3]$.

These data can be used directly to compute the generalized aerodynamic-force matrices (GAF) and run flutter analyses. Moreover, they are used to generate sinusoidal time signals as training

Table 1: Mode table

Index	name	vacuum frequency
1	1st bending vertical	$0.80\,Hz$
2	2nd bending vertical	$2.04\,Hz$
3	1st in-plane bending	$2.20\,Hz$
4	engine vertical	$2.25\,Hz$
5	3rd bending vertical	$4.32\,Hz$
6	2nd in-plane bending	$5.26\,Hz$
7	4th bending vertical	$6.85\,Hz$
8	5th bending vertical	$7.56\,Hz$
9	1st torsion	$9.20\,Hz$
10	3rd in-plane bending	$10.67\,Hz$
11	higher bending vertical	$11.62\,Hz$
12	2nd torsion	$14.45\,Hz$

Table 2: Flow conditions

Parameter	value
Mach number	0.85
Density	$0.457\,kg/m^3$
Pressure	$30\,kPa$
Temperature	$229.4\,K$
Velocity	$258\,m/s$
Reynolds number	$3.94e5$
Reynolds reference length	$1\,m$
Steady lift coefficient (rigid)	0.5014
Steady lift coefficient (flexible)	0.2123

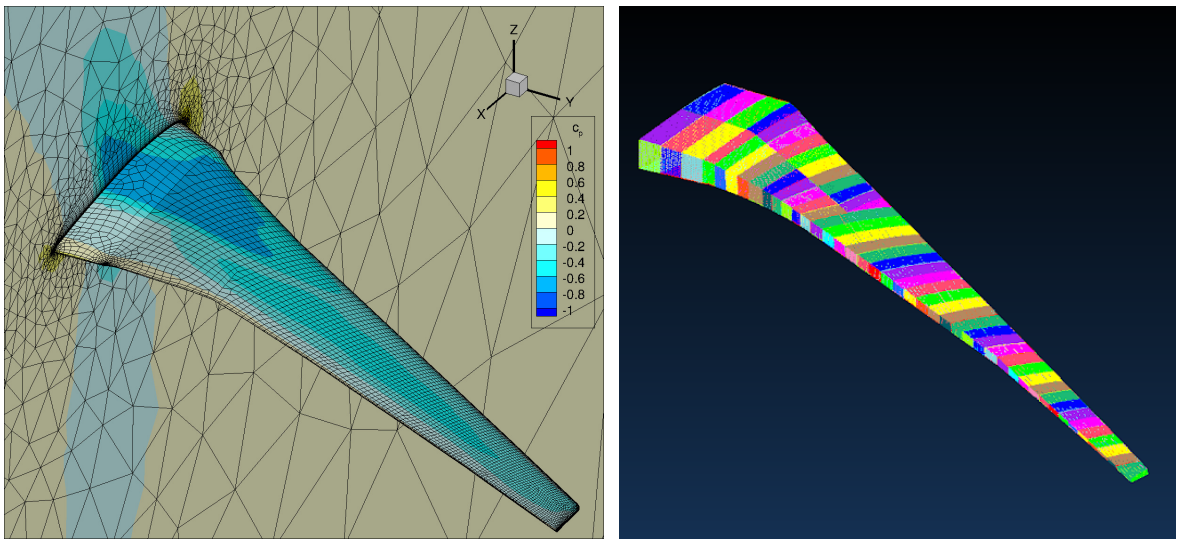

(a) CFD model with steady pressure coefficient (b) FE model

Figure 3: High aspect ratio wing

inputs for the auto-encoder-transformer network. The network is then used to predict unsteady pressures for various sinusoidal excitations and the GAF matrices can be computed via Fourier transformation.

4 RESULTS

The combination of auto-encoder and transformer is demonstrated in two steps. In the first step, the auto-encoder is used on the training data to directly analyze its compression loss. In the second step, the transformer is trained on the latent-space response and evaluated on the same training sets as well as on additional frequencies that were not part of the training.

The presented flutter results are computed with an in-house p-k method using a constant Mach number and a single input of the GAF matrix. Thus, varying speed corresponds to varying flight level and the aerodynamic influence is changed only through the dynamic pressure as a factor to the GAF.

4.1 Auto-Encoder

In Figure 4 the effect of the auto-encoder on the flutter predictions is demonstrated for 3 different latent-space sizes: $48, 24$ and 12 while the shrink factor was kept constant at 0.4. Here, the LFD data were transformed into the time-domain with every 16th time-step used as a training input for the auto-encoder. Afterwards, the complete auto-encoder, i.e. encoder and decoder, was applied to all time-domain data and transferred back into the frequency domain allowing to analyze the loss due to the data compression, separately. An excellent agreement to the

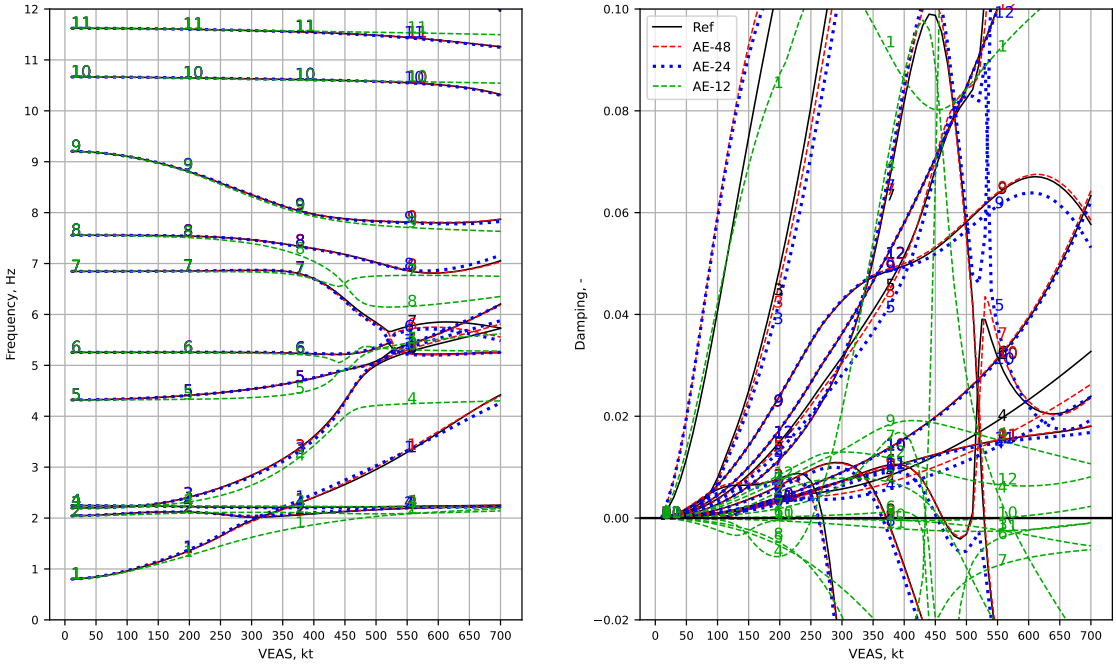

Figure 4: Effect of auto-encoder on flutter results for different latent-space size

reference is obtained using a latent-space size of 48 whereas small deviations can be observed for a size of 24. compressing the data even further to size of 12 results in large deviations in the damping prediction for several modes that are not related to the reference at all.

In the follow-up analyses, the auto-encoder with latent-space size of 48 is used. The unsteady local pressures are compared in Figure 5 for the second bending mode, subplot (a), and for the first torsion mode in subplot (b). Very good agreement is obtained on both span stations for the torsion mode, whereas small differences can be observed for the second bending mode. However, the unsteady response due to the second bending is significantly smaller than the response due to torsion explaining these deviations. The same explanation holds for the observation, that

the deviations at the inner span station are larger compared to the outer span station.

4.2 Auto-Encoder and Transformer on training set

After the auto-encoder has been checked, the training data are transformed into the latent subspace and a transformer network is trained connecting a time-window of excitations to the next prediction of encoded c_p. The obtained transformer is evaluated at the same frequencies as the training inputs and the results are transferred into the frequency domain to compute the GAF matrices. In Figure 6 the frequency response function of diagonal elements of the GAF matrix is shown. In general, a good agreement is obtained between the ML model and it's direct LFD counterpart. Small deviations can be seen especially for the phase of the sixth mode, the second in-plane bending. However, the response is relatively small compared to the other modes. The effect on the flutter prediction is shown in Figure 7 demonstrating a comparable agreement to the direct LFD results as with the auto-encoder only as shown in Figure 4.

4.3 Auto-Encoder and Transformer on test set

After it was ensured that the ML model can reproduce the training data sufficiently accurate, the model is evaluated at different reduced frequencies not part of the training data. The frequency responses of GAF entries $(2,2), (5,5), (6,6)$ and $(7,7)$ are shown in Figure 8. Except for the wiggles observed in the phase of the second in-plane bending (mode 6), excellent agreement is obtained. Because of this good comparison, it is not surprising that the flutter predictions agree similarly well, shown in Figure 9. Lastly, the local surface pressure coefficients are compared in Figure 10 yielding a good agreement. Especially for the torsion mode, excellent agreement is obtained with small deviations only at the inner wing region which contributes significantly less to the overall GAF in comparison with the outer wing. The differences for the bending mode are larger, however, at a smaller scale compared to the torsion.

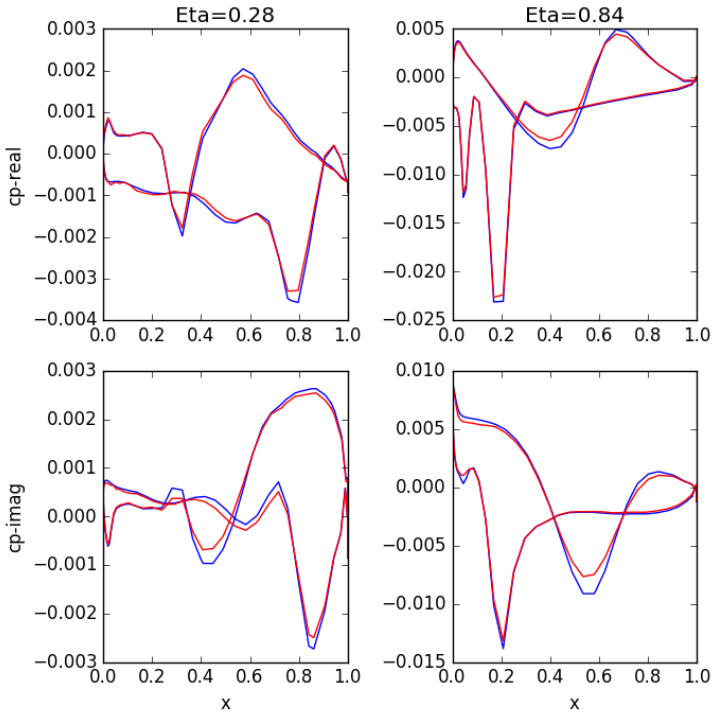

(a) second vertical bending, $\omega^* = 0.2$

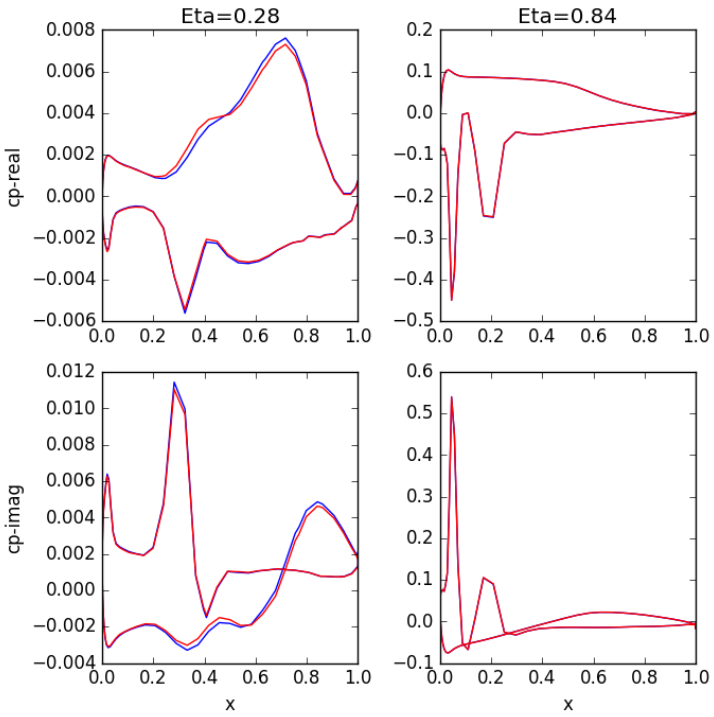

(b) first torsion, $\omega^* = 0.1$

Figure 5: Effect of auto-encoder on local pressure coefficient

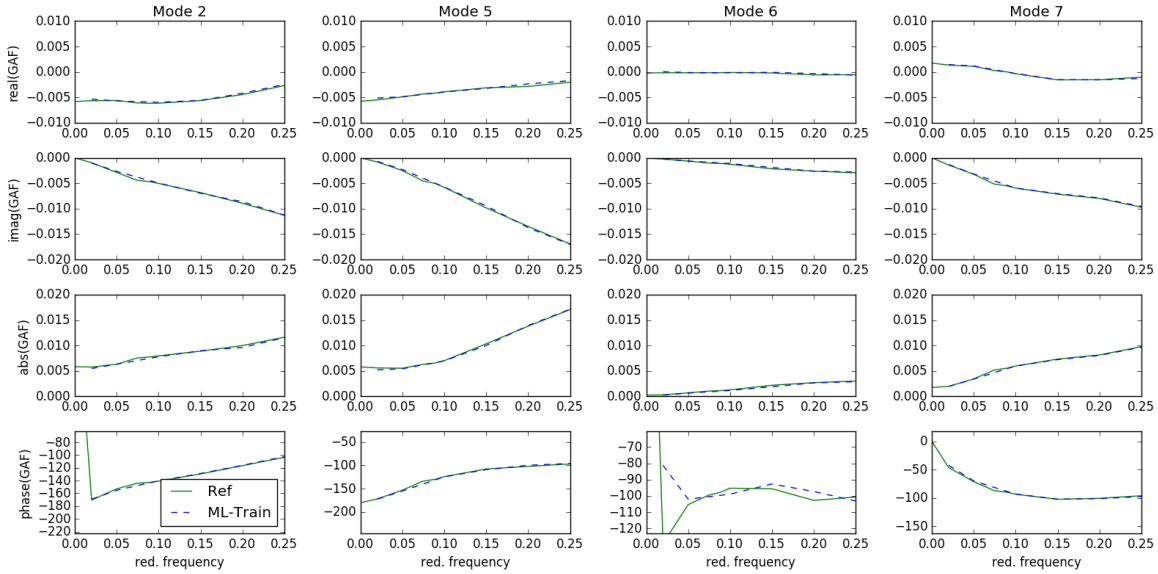

Figure 6: Frequency response function of the GAF main diagonal element of auto-encoder-transformer network on training set

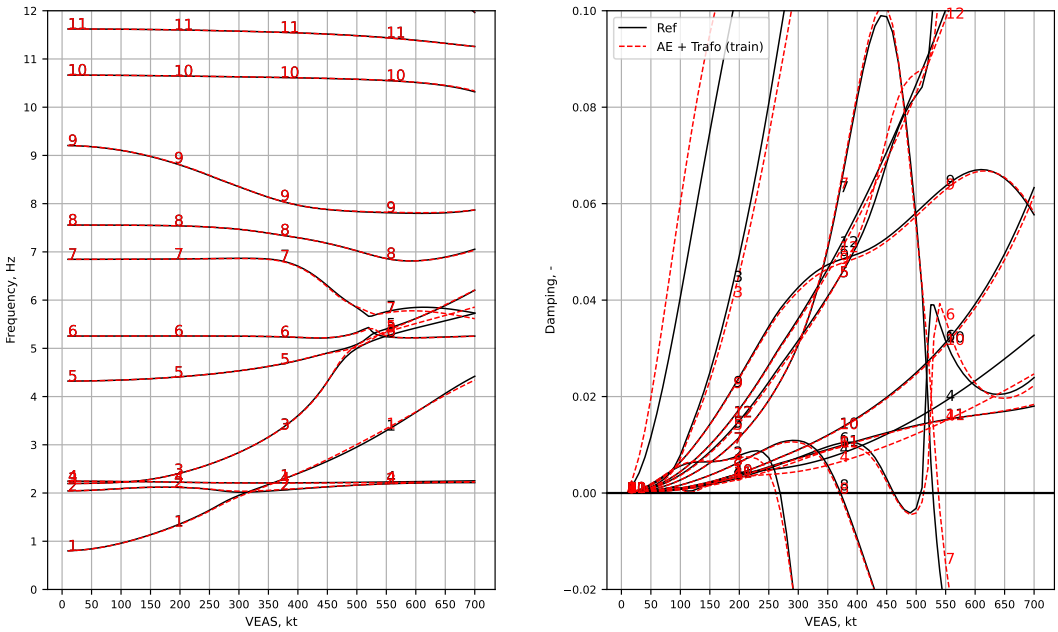

Figure 7: Effect of neural network on flutter results on training set

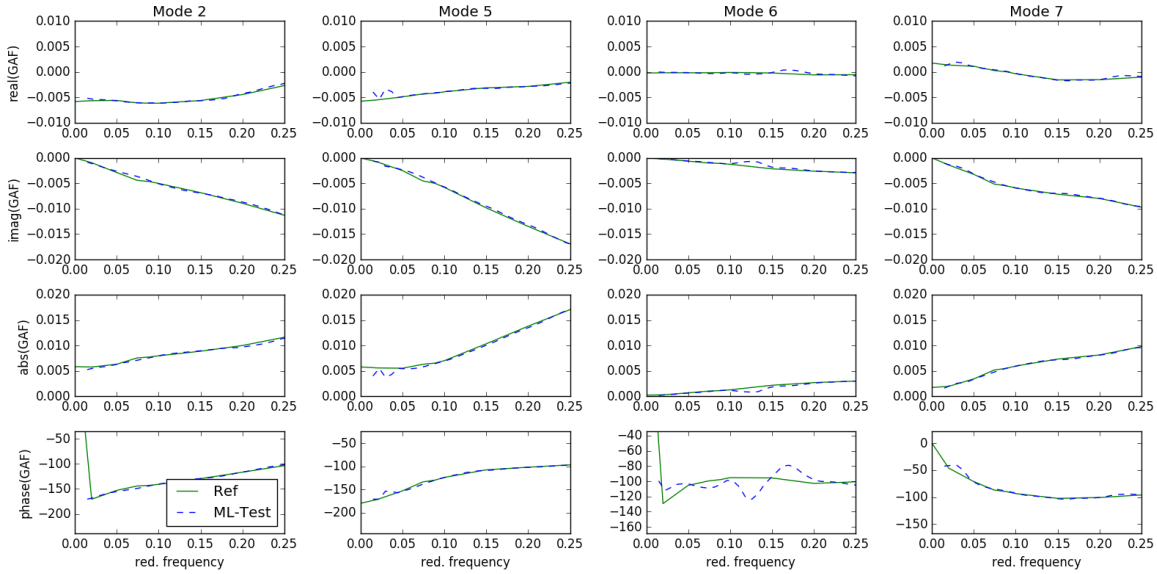

Figure 8: Frequency response function of the GAF main diagonal element of auto-encoder-transformer network on test set

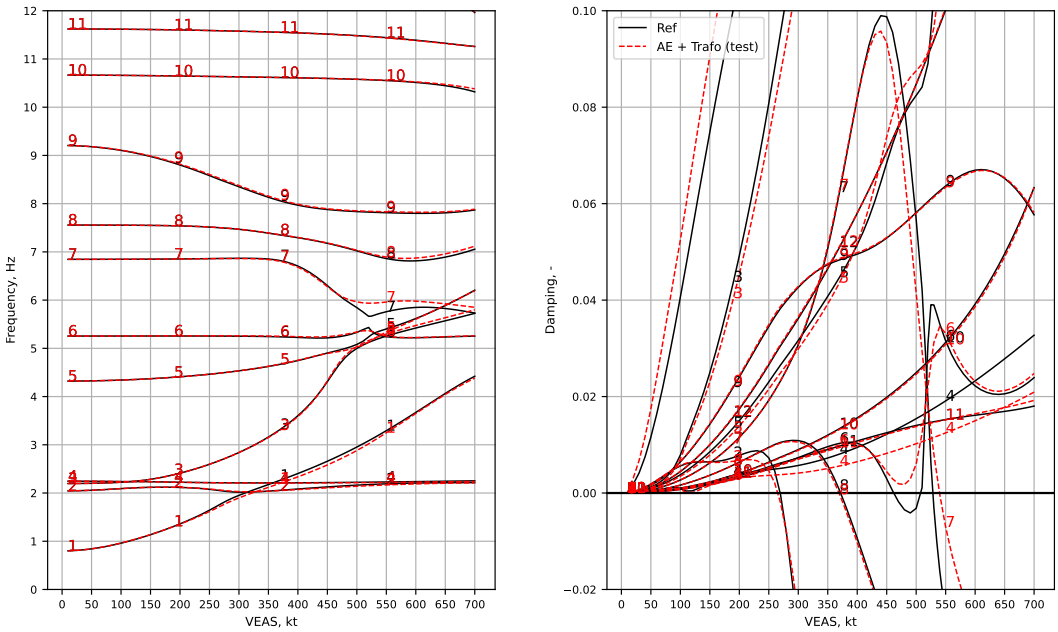

Figure 9: Effect of neural network on flutter results on test set

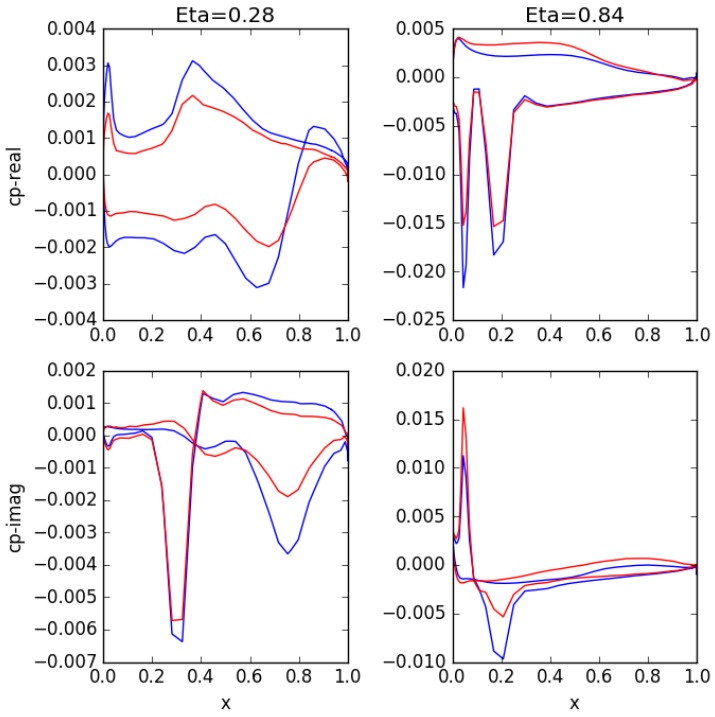

(a) second vertical bending, $\omega^* = 0.074$

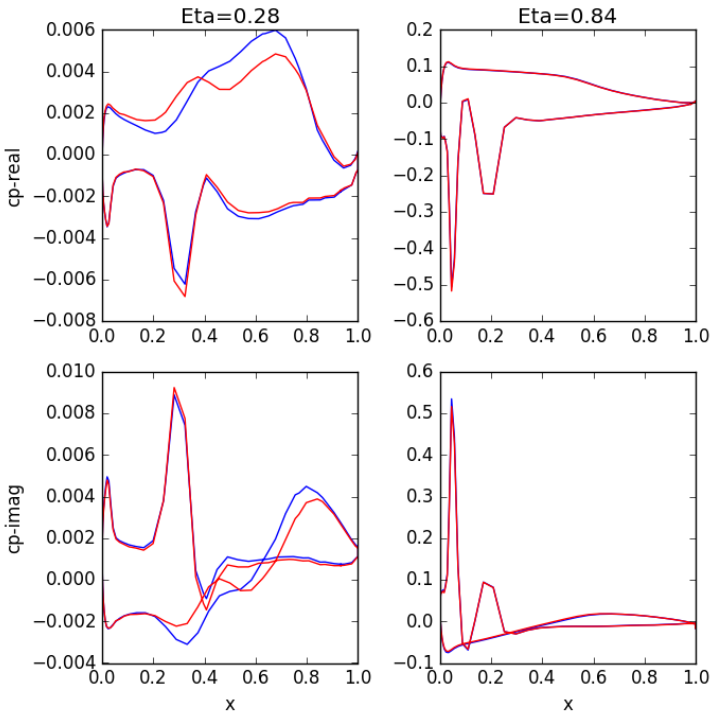

(b) first torsion, $\omega^* = 0.089$

Figure 10: Predicted local pressure coefficient on test set

5 CONCLUSION

In this paper, the combination of an auto-encoder coupled with a transformer is presented to predict unsteady surface pressures due to forced excitation. While the used neural-network architecture operates in the time domain, training data are computed with the linearized, frequency-domain CFD solver for a generic, high-aspect-ratio wing. These data are transfered into the time-domain to train the network, while the network's outputs are Fourier transformed and compared to their corresponding reference.

Results are shown for unsteady, local surface pressure coefficients as well as for frequency response functions of entries of the generalized aerodynamic force matrix. Throughout the work, a good agreement is demonstrated, showing deviations mainly in the inner wing section and the contribution of the inner wing on the overall forces is small. Excellent agreement is obtained for the outer wing section, especially for the torsion mode whereas mode shapes with smaller contribution to the generalized aerodynamic force matrix show small differences. The data are used to perform flutter analysis confirming the accuracy of the presented neural network.

Future developments will focus on introducing nonlinearities in form of different linearization points, e.g. LFD data computed for different speeds/dynamic pressures, and on introducing amplitude nonlinearities to support the analysis of limit-cycle oscillations. In [10], a next level of complexity has been introduced with a reduced-order model framework for the simulation of surface aerodynamic quantities. This framework embeds graph networks with a implemented multi-mesh scheme. This approach enables a better reconstruction of the aerodynamic fields from a spatial discretization. This analysis is another promising opportunity to improve the predicting quality of data-driven neural networks.

6 REFERENCES

[1] Wang, Q., Medeiros, R., Cesnik, C., et al. (2019). Techniques for improving neural network-based aerodynamics reduced-order models. In *AIAA-2019-1849*. doi: 10.2514/6.2019-1849.

[2] Wang, Q., Cesnik, C., and Fidkowski, K. J. (2020). Multivariate recurrent neural network models for scalar and distribution predictions in unsteady aerodynamics. In *AIAA-2020-1533*. doi:10.2514/6.2020-1533.

[3] Ribeiro, M. D., Stradtner, M., and Bekemeyer, P. (2023). Unsteady reduced order model with neural networks and flight-physics-based regularization for aerodynamic applications. In *Computers & Fluids*, vol. 264.

[4] Bekemeyer, P., Bertram, A., Chaves, D. A. H., et al. (2022). Data-driven aerodynamic modeling using the DLR SMARTy toolbox. In *AIAA AVIATION 2022 Forum, American Institute of Aeronautics and Astronautics*. Reston, Virginia. doi:10.2514/6.2022-3899.

[5] Vaswani, A., Shazeer, N., Parmar, N., et al. (2017). Attention is all you need. *CoRR*, abs/1706.03762.

[6] Thormann, R. and Widhalm, M. (2013). Linear-frequency-domain predictions of dynamic-response data for viscous transonic flows. *AIAA Journal*, 51(11), 2540–2557. doi:10.2514/1.J051896.

[7] Gerhold, T. and Galle, M. (1997). Calculation of complex three-dimensional configurations employing the DLR TAU-code. In *AIAA Paper 97-0167*.

[8] Spalart, P. and Allmaras, S. R. (1992). A one-equation turbulence model for aerodynamic flows. In *AIAA Paper 92-0439*.

[9] Stickan, B. (2018). *Explanation of AEROSTABIL limit-cycle oscillations via high-fidelity aeroelastic simulations*. Ph.D. thesis.

[10] Massegur, D. and Ronch, A. D. (2023). Recurrent multi-mesh convolutional autoencoder framework for spatio-temporal aerodynamic modelling. In *Computers & Fluids*, vol. 264.

COPYRIGHT STATEMENT